ChemPubSoc Europe

DOI: 10.1002/ejic.201500873

EurJIC
European Journal of Inorganic Chemistry

Full Paper

CLUSTER ISSUE

Phosphaferrocene Derivatives

The First Coordination Polymers Based on 1,3-Diphosphaferrocenes and 1,1′,2,3′,4-Pentaphosphaferrocenes

Claudia Heindl,[a] Sabine Reisinger,[a] Christoph Schwarzmaier,[a] Lena Rummel,[a] Alexander V. Virovets,[b,c] Eugenia V. Peresypkina,[b,c] and Manfred Scheer*[a]

Dedicated to Professor Heinrich Lang on the occasion of his 60th birthday

Abstract: Phosphaferrocenes in combination with coinage metal salts proved to be excellent building blocks in supramolecular chemistry for the buildup of oligomeric and polymeric assemblies. The synthesis of a series of novel phosphaferrocenes containing the 1,3-$P_2C_3iPr_3$ and/or the 1,2,4-$P_3C_2iPr_2$ ligand is described herein. The self-assembly processes of the 1,3-diphospha-, 1,2,4-triphospha-, and 1,1′,2,3′,4-pentaphosphaferrocenes with Cu^I halides led to the formation of 1D or 2D polymers. With $[Cp^*Fe(\eta^5\text{-}P_2C_3iPr_3)]$ ($Cp^* = \eta^5\text{-}C_5Me_5$), infinite chains are formed, whereas with $[(\eta^5\text{-}P_3C_2iPr_2)Fe(\eta^5\text{-}P_2C_3iPr_3)]$ 1D ladderlike structures are obtained. These are the first polymers containing such a di- and pentaphosphaferrocene, respectively. On the other hand, the use of $[Cp^*Fe(\eta^5\text{-}P_3C_2iPr_2)]$ leads to the construction of 2D networks with intact sandwich complexes, which is uncommon for this class of complexes.

Introduction

The year 2016 marks the 50th anniversary of 2,4,6-triphenylphosphabenzene, and until now the fundamental interest in main group heterocycles is unabated.[1] According to the isolobal principle, the formal substitution of methine moieties in aromatic rings (e.g., benzene, cyclopentadienide) by substituent-free phosphorus atoms is possible. The resulting derivatives of Cp^- are also capable of acting as η^5 ligands for the synthesis of sandwich complexes, classified as phosphametallocenes. Among them, the phosphaferrocenes containing iron and one to six P atoms are the most popular representatives. First labeled as "laboratory curiosity",[2] their widespread potential in catalysis and supramolecular chemistry soon was recognized. Contrary to their all-carbon analogue, the lone pairs of the phosphorus atoms make them excellent building blocks towards Lewis acidic metal salts. We especially use Cu^I halides as linker molecules, since they show great versatility in combination with phosphaferrocenes.

The 1,2,3,4,5-pentaphosphaferrocene $[Cp^*Fe(\eta^5\text{-}P_5)]$ ($Cp^* = \eta^5\text{-}C_5Me_5$), for instance, is capable of building up polymeric[3] or, depending on the applied conditions, even spherical coordination compounds.[4] These sensitive self-assembly processes also depend on the substitution patterns of the phosphaferrocenes. Especially 1,2,4-triphosphaferrocenes $[Cp^RFe(\eta^5\text{-}P_3C_2R'_2)]$ (Cp^R = Cp, Cp*, Cp‴; $Cp''' = \eta^5\text{-}C_5H_2tBu_3$; R′ = tBu, Ph, Mes) have been synthesized and studied extensively concerning their coordination potential (Figure 1, a–c).[5] Thereby, special attention is paid to the influence of the substitution pattern on the coordination behavior towards Cu^I halides. For example, the 1,2,4-triphosphaferrocenes $[Cp^RFe(\eta^5\text{-}P_3C_2tBu_2)]$ (Cp^R = Cp, Cp*) form dimeric (Figure 1, a) and oligomeric products with stoichiometric amounts of CuX (X = Cl, Br, I), and in one case a 2D polymer with an excess of CuI.[6] The last-named example is the only coordination polymer containing an intact 1,2,4-triphosphaferrocene complex. On the other hand, an astonishing fragmentation and rearrangement process to form a tetraphosphabutadiene ligand can be observed with the Cp‴ complex $[Cp'''Fe(\eta^5\text{-}P_3C_2tBu_2)]$ (Figure 1, b).[7]

Furthermore, especially the R′ group at the phospholyl ligand profoundly affects its reactivity. Thus, enhancement of the steric bulk at the phospholyl ring results in completely different reactivity: The combination of the mesityl-substituted phosphaferrocene $[Cp^*Fe(\eta^5\text{-}P_3C_2Mes_2)]$ with CuX (X = Cl, Br, I) entails fragmentation of the sandwich complex. The split-off $[P_3C_2Mes_2]^-$ ligand serves as building block for the formation of oligomeric and polymeric assemblies (Figure 1, c).[8]

Therefore, large substituents at the Cp^R or phospholyl ligand lead to a higher instability of the phosphaferrocenes with respect to fragmentation. Encouraged by these results, we were particularly interested in decreasing the steric demand of the

---

[a] Institut für Anorganische Chemie, Universität Regensburg,
93040 Regensburg, Germany
E-mail: Manfred.scheer@ur.de
http://www.uni-regensburg.de/chemie-pharmazie/anorganische-chemie-scheer/

[b] Nikolaev Institute of Inorganic Chemistry, Siberian Division of RAS,
Acad. Lavrentyev str. 3, 630090 Novosibirsk, Russia

[c] Novosibirsk State University,
Pirogova str., 2, 630090 Novosibirsk, Russia

Supporting Information for this article is available on the WWW under http://dx.doi.org/10.1002/ejic.201500873.

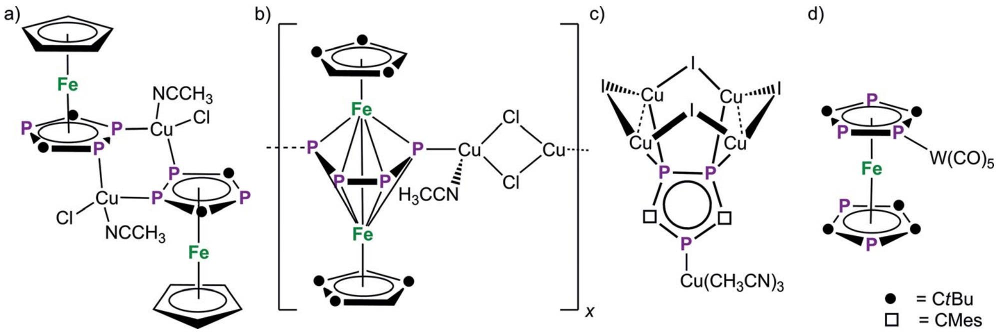

Figure 1. Selected examples of coordination products of 1,2,4-triphosphaferrocenes with Cu^I halides (a–c) and a 1,1′,2,3′,4-pentaphosphaferrocene with a $\{W(CO)_5\}$ fragment (d).

R′ group in the phospholyl ligand, which has been neglected so far. For this purpose, the smaller *i*Pr substituent moved into our focus. The less bulky ligand may enhance the stability of the corresponding phosphaferrocenes and thus allow coordination chemistry without fragmentation and rearrangement processes. The common synthetic route for the preparation of $[P_3C_2R'_2]^-$ starts from the corresponding phosphaalkene[5d] or phosphaalkyne[9] and is accompanied by the formation of $[P_2C_3R'_3]^-$ as a byproduct (Scheme 1).

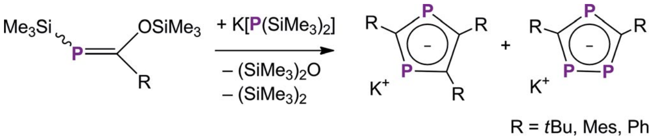

Scheme 1. Established synthesis of 1,3-di- and 1,2,4-triphospholyl moieties.

Concerning the *i*Pr group, Nixon et al. showed that treating a mixture of the phosphaalkynes *i*PrC≡P and *t*BuC≡P with sodium results in the formation of nine differently substituted 1,3-di- and 1,2,4-triphospholyl ligands.[9] Though several derivatives of 1,3-diphospholyl ligands were synthesized by this method, no comprehensive coordination studies involving these heterocycles are known in the literature. Merely a few phosphaferrocenes are structurally characterized: two 1,3-diphosphaferrocenes $[Cp^RFe(\eta^5\text{-}P_2C_3R'_3)]$,[5f,10] four 1,1′,3,3′-tetraphosphaferrocenes $[(\eta^5\text{-}P_2C_3R'_3)_2Fe]$,[11] and one 1,1′,2,3′,4-pentaphosphaferrocene $[(\eta^5\text{-}P_3C_2tBu_2)Fe(\eta^5\text{-}P_2C_3tBu_3)]$.[12] In addition, the last-named sandwich complex has been used for coordination of a $\{W(CO)_5\}$ fragment (Figure 1, d)[13] and a ligand-transfer reaction.[14] Furthermore, Nixon et al. described mass-spectrometric evidence of the *i*Pr derivatives of these three phosphaferrocenes among a mixture of more than 20 different sandwich complexes.[9] No supramolecular assemblies based on phosphaferrocenes containing a 1,3-diphospholyl ligand are known.

Herein, we report on the straightforward synthesis and characterization of a series of partly hitherto unknown phosphaferrocenes containing the *i*Pr-substituted phospholyl ligands 1,3-$[P_2C_3iPr_3]$ and 1,2,4-$[P_3C_2iPr_2]$. The 1,3-di-, 1,2,4-tri-, and 1,1′,2,3′,4-pentaphosphaferrocene were further used as building blocks in coordination chemistry with Cu^I halides. Reactions with the 1,2,4-triphosphaferrocene allowed the isolation of novel 2D polymeric networks. On the other hand, the use of $[Cp^*Fe(\eta^5\text{-}P_2C_3R'_3)]$ and $[(\eta^5\text{-}P_3C_2tBu_2)Fe(\eta^5\text{-}P_2C_3tBu_3)]$ led to the formation of 1D chains, which are the first coordination polymers containing this type of di- and pentaphosphaferrocenes, respectively.

Results and Discussion

Synthesis and Characterization of the Phosphaferrocenes

The preparation of the phospholyl salts $K[P_2C_3iPr_3]$ (**1a**) and $K[P_3C_2iPr_2]$ (**1b**) was carried out analogously to the *t*Bu derivative[5d,15] starting from the corresponding phosphaalkene $Me_3SiO(iPr)C{=}P(SiMe_3)$[16] and $KP(SiMe_3)_2$ (cf. Scheme 1 for R = *i*Pr).[17] In contrast, Nixon et al. treated the phosphaalkyne with elemental sodium to obtain the sodium derivatives of **1a** and **1b** among other products.[9] Interestingly, the product distribution of **1a** and **1b** turned out to be temperature-dependent. According to $^{31}P\{^1H\}$ NMR spectroscopy after 1 d of heating at 50 °C, the ratio **1a**/**1b** is about 1:1. After isolation of this first crop of product the remaining mother liquor was heated for a further day to favor the formation of **1b** (**1a**/**1b** = 0.75:1). When the reaction mixture was finally heated to reflux at 100 °C, the last crop of the isolated off-white powder solely contained the triphospholyl salt **1b**. Therefore, a selective synthesis of **1b** at least is feasible. Since both salts are needed for the subsequent reaction, the initial solution was heated to 75 °C for 3 d instead to give **1a** and **1b** in approximately 1:1 ratio.

The $^{31}P\{^1H\}$ NMR spectrum of the isolated product in $[D_8]$thf shows a singlet at $\delta = 159.6$ ppm, which can be assigned to **1a** (cf. $Na[P_2C_3iPr_3]$: $\delta = 155.0$ ppm).[9] Surprisingly, for **1b** a doublet of doublets at $\delta = 247.6$ ppm ($^2J_{PP} = 51.6$ and 45.1 Hz) and a pseudodoublet ($\delta = 244.7$ ppm) with a merged coupling constant of $^2J_{PP} = 49.0$ Hz were observed for the isolated and the adjacent phosphorus atoms, respectively. For comparison, previously reported derivatives $[1,2,4\text{-}P_3C_2R_2]^-$ all show a (slightly low-field shifted) doublet and triplet with a similar coupling constant (R = Mes:[5a] $\delta = 266.4, 261.7$ ppm, $^2J_{PP} = 38$ Hz; R = Ph,[5a] $\delta = 274.4, 253.9$ ppm, $^2J_{PP} = 43$ Hz; R = *t*Bu:[5b] $\delta = 256, 248$ ppm, $^2J_{PP} = 49$ Hz). For $Na[P_3C_2iPr_2]$, a slight high-field shift compared to **1b** was observed ($\delta = 241.6$ and 246.6 ppm, $^2J_{PP} = 48$ Hz).[9]

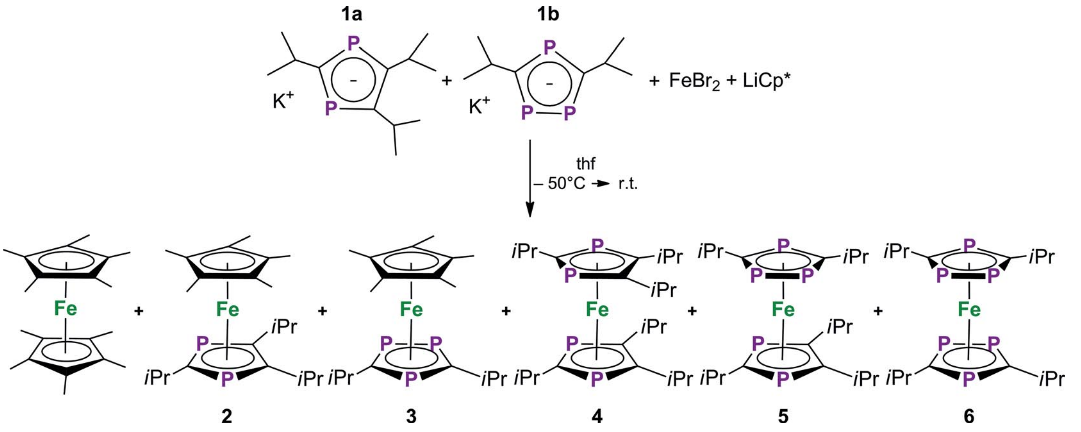

Scheme 2. Synthesis of phosphaferrocenes **2**–**6**.

For the subsequent synthesis of the novel 1,3-diphospha ferrocene [Cp*Fe(η^5-P_2C_3*i*Pr$_3$)] (**2**) and 1,2,4-triphosphaferrocene [Cp*Fe(η^5-P_3C_2*i*Pr$_2$)] (**3**) we also referred to the established strategy for the *t*Bu derivative.[5k] Thus, solutions of FeBr$_2$(dme) and LiCp* in thf were added to a mixture of **1a** and **1b** in thf at –50 °C (Scheme 2), and an immediate color change from orange to deep reddish brown resulted. $^{31}P\{^1H\}$ and ^1H NMR spectroscopic investigations of the crude reaction mixture revealed signals corresponding to **2** and **3**, but also signals of small amounts of byproducts. These included [Cp*$_2$Fe], the 1,1′,3,3′-tetraphosphaferrocene [(η^5-P_2C_3*i*Pr$_3$)$_2$Fe] (**4**), the 1,1′,2,3′,4-pentaphosphaferrocene [(η^5-P_3C_2*i*Pr$_2$)Fe(η^5-P_2C_3*i*Pr$_3$)] (**5**), and the 1,1′,2,2′,4,4′-hexaphosphaferrocene [(η^5-P_3C_2*i*Pr$_2$)$_2$Fe] (**6**). The sandwich complexes **5** and **6** were already reported but only characterized by mass spectrometry in a mixture of more than 20 phosphaferrocenes.[9]

The phosphaferrocenes were separated by an elaborate column-chromatographic workup. A yellow band of [Cp*$_2$Fe], followed by a green fraction of a mixture of **4**, **5**, and **6** was eluted with hexane. With a slightly more polar eluent (hexane/toluene = 10:1) a red band of a mixture of **2** and **3** was obtained. For the isolation of the pure phosphaferrocenes, further column-chromatographic workup of the green and red fractions is necessary (see Supporting Information and Exp. Section). In this way, analytically pure compounds **2**, **3**, and **5** were obtained.

All phosphaferrocenes were identified by their characteristic chemical shifts and multiplicity in the ^1H and $^{31}P\{^1H\}$ NMR spectra. Compared to those of **1a** and **1b**, the P atoms show a significant high-field shift of more than 100 ppm in the corresponding $^{31}P\{^1H\}$ NMR spectra, which is a usual trend in phosphaferrocene chemistry.[5a,5f,12,18] In contrast to **1b** and in analogy to known 1,2,4-triphospholyl derivatives, the P_3C_2 rings all show a doublet and a triplet for the isolated and adjacent phosphorus atoms on coordination to iron, respectively ($^2J_{PP}$ = 43.8 Hz in **3**, 42.0 Hz in **5**, and 38.0 Hz in **6**) (Table 1). On the other hand, a singlet is obtained for the P_2C_3 ligands. In addition, multiplets in the range of δ = 2.2–3.1 ppm in the ^1H NMR spectra can be assigned to the methine groups, whereas all methyl groups show doublets ($^3J_{HH}$ = 6.1–6.7 Hz) with chemical shifts between 1.0 and 1.7 ppm (for detailed assignment, see Exp. Section). In ferrocenes containing the 1,3-diphospholyl ring, two sets of signals are observed for the CH units (integral ratio: 1:2) and three for the CH_3 groups (1:1:1). For the 1,2,4-triphospholyl moieties in **3**, **5**, and **6**, one multiplet (CH) and two doublets (CH_3) per ring are monitored.

Table 1. $^{31}P\{^1H\}$ chemical shifts δ [ppm] of **2**–**5** in C_6D_6 at room temperature and of **6** in CD_2Cl_2 at 193 K.

	δ [ppm] (P_2C_3)	δ [ppm] (P_3C_2)	$^2J_{PP}$ [Hz]
1a	161.4 (s)		
1b		247.6 (dd), 244.7 (pseudo-d)	51.6, 45.1, 49.0
2	–2.8 (s)	–	–
3	–	29.7 (t), 49.6 (d)	43.8
4	6.7 (s)	–	–
5	15.0 (s)	46.9 (t), 53.7 (d)	42.0
6	–	46.2 (d), 69.3 (t)	38.0

In the FD mass spectra the molecular-ion peaks are observed for all complexes **2**–**6**, albeit with low intensity for **4**. In addition, the structures of **2**, **4**, and **5** were confirmed by X-ray structural analyses (see below).

Molecular Structures of 2, 4, and 5

Crystals of **2**, **4**, and **5** suitable for X-ray structural analysis were obtained by layering toluene solutions with CH_3CN and storing at –28 °C (Figure 2). Compound **2** crystallizes in the monoclinic space group $P2_1/c$, **4** in the triclinic space group $P\bar{1}$, and **5** in three monoclinic polymorphic modifications ($P2_1$, $P2_1/n$, for details see Supporting Information and Table 3). All molecular structures can be described as sandwich complexes with η^5-coordinated ligands in an eclipsed conformation. The tetraphosphaferrocene **4** forms the most "perfect" sandwich complex with an interplanar angle of 0.27(5)° and a (P_2C_3*i*Pr$_3$)$_{centroid}$–Fe–(P_2C_3*i*Pr$_3$)$_{centroid}$ angle of 179.84(2)°. These distortions are slightly more pronounced in **2** [3.33(7)° and 177.09(3)°] and **5** [3.57(7)° and 177.25(3)°] (Figure 2). The interplanar angles are comparable to those of the *t*Bu-substituted 1,2,4-triphosphaferrocenes [Cp^{R}Fe(η^5-P_3C_2*t*Bu$_2$)] (2.2° for Cp^R = Cp; 0.1° for Cp^R =

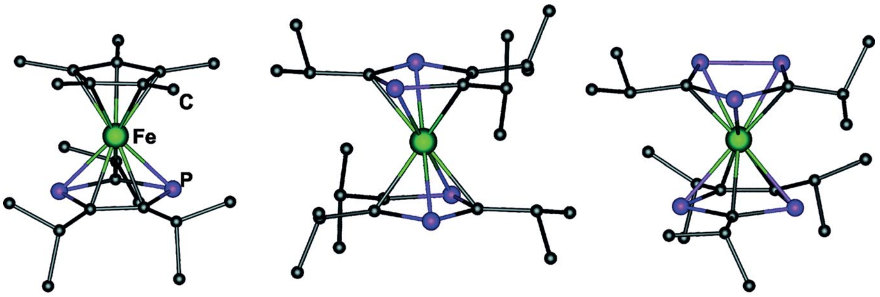

2 **4** **5**

Figure 2. Molecular structures of the phosphaferrocenes **2**, **4**, and **5**. H atoms are omitted for clarity.

Cp‴)[7,5d] and much smaller than that in the tilted [Cp*Fe(η^5-$P_3C_2Mes_2$)] derivative (12.2°).[5a] Thus, dissociation of the cyclopentadienyl[19] or the phospholyl ligand[8] is rather unlikely.

Within the coordinated di- and triphospholyl rings, all bond lengths lie between those of a single and a double bond and thus confirm the aromaticity of this ligand (Table 2; sums of covalent radii: C–C: 1.50 Å; C–P: 1.86 Å; P–P: 2.22 Å; C=C: 1.34 Å; C=P: 1.69 Å; P=P: 2.04 Å).[20]

Table 2. Selected bond lengths [Å] within the phospholyl rings in **2**, **4**, **5**, **5′**, and **5″**. Ranges of bond lengths are given if more than one bond is present in the asymmetric unit.

	Ligand	P–P	P–C	C–C
2	P_2C_3	–	1.761(2)–1.784(2)	1.424(2)–1.426(3)
4	P_2C_3	–	1.770(2)–1.789(2)	1.425(3)–1.430(3)
5	P_2C_3	–	1.759(5)–1.790(6)	1.438(7)–1.440(7)
	P_3C_2	2.121(2)–2.134(2)	1.746(5)–1.777(5)	–
5′	P_2C_3	–	1.763(1)–1.786(1)	1.419(2)
	P_3C_2	2.126(1)	1.759(2)–1.769(2)	–
5″	P_2C_3	–	1.756(3)–1.794(3)	1.441(4)–1.445(3)
	P_3C_2	2.119(1)–2.121(1)	1.761(3)–1.772(3)	–

Diphosphaferrocene 2 as Building Block

Although 1,3-diposphaferrocenes have been known since 1990,[10] they have not yet been used for the formation of supramolecular assemblies. However, the separate and therefore opposite positions of the phosphorus atoms in the ring are predestinated for the buildup of 1D coordination polymers. Hence, diffusion experiments of **2** with CuX (X = Br, I) were carried out and led to the crystallization of [{Cp*Fe(μ_3,$\eta^{5:1:1}$-$P_2C_3iPr_3$)}$Cu_2(\mu$-$Br)_2(CH_3CN)]_n$·$0.75n(CH_3CN)$ (**2**-Br) and [{Cp*Fe(μ_3,$\eta^{5:1:1}$-$P_2C_3iPr_3$)}$Cu_2(\mu$-$I)_2(CH_3CN)_{0.5}]_n$·$0.5n(CH_3CN)$ (**2**-I), respectively (Scheme 3).

Compound **2**-Br crystallizes as orange platelets in the monoclinic space group *C2/c*, whereas **2**-I crystallizes in the orthorhombic space group $P2_12_12_1$ (for crystallographic data see Table 3 for **2**-Br and Table 4 for **2**-I). The X-ray structural analyses revealed that, in both **2**-Br and **2**-I, 1D chains are formed from moieties of **2** linked by {$Cu_2(\mu$-$X)_2$} four-membered rings (Figure 3, for bond lengths see Supporting Information).

The bending of the strands is caused by the position of the phosphorus atoms within the P_2C_3 five-membered ring and the tetrahedral coordination environment of some of the copper ions. The latter makes the difference between the iodine and the bromine derivative: At first, they differ in their numbers of acetonitrile ligands, coordination of which leads to expansion of the environment of the copper center from trigonal planar to tetrahedral. In **2**-Br, every second Cu atom is affected and thus all {$Cu_2(\mu$-$Br)_2(CH_3CN)$} rings are similar. On the contrary, the iodine analogue **2**-I contains fewer acetonitrile ligands, and only every fourth Cu atom is four-coordinated.

Consequently, the {$Cu_2(\mu$-$I)_2$} and {$Cu_2(\mu$-$I)_2(CH_3CN)$} units are perpendicular to each other. This results in a different undulation of the chains. Furthermore, the phosphaferrocene units in **2**-Br are oriented upwards and downwards in alternation. In contrast, this change in direction occurs only after every second moiety of **2** in **2**-I (Figure 3). Unfortunately, an unambiguous

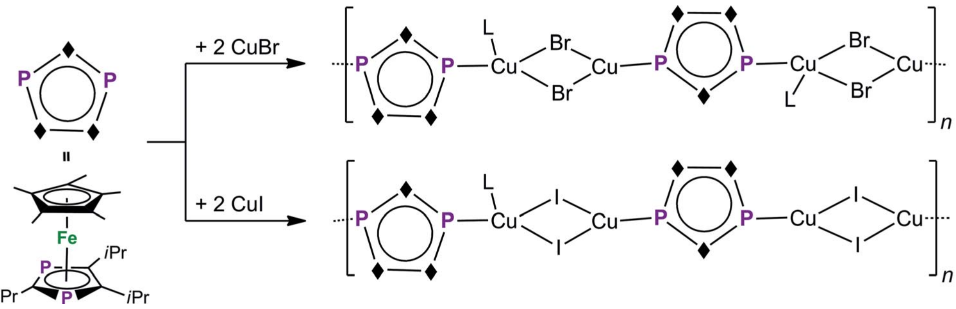

2-Br

2-I

Scheme 3. 1,3-Diphosphaferrocene-derived coordination polymers **2**-Br and **2**-I.

Table 3. Crystallographic data for **2**, **4**, **5**, **5′**, **5″**, and **2**-Br.

	2	**4**	**5**	**5′**	**5″**	**2**-Br
Formula	$C_{22}H_{36}FeP_2$	$C_{24}H_{42}FeP_4$	$C_{20}H_{35}FeP_5$	$C_{20}H_{35}FeP_5$	$C_{20}H_{35}FeP_5$	$C_{24}H_{39}Br_2Cu_2FeNP_2\cdot 0.75(CH_3CN)$
FW	418.30	510.31	486.18	486.18	486.18	777.04
Crystal system, space group	monoclinic, $P2_1/c$	triclinic, $P\bar{1}$	monoclinic, $P2_1$	monoclinic, $P2_1/n$	monoclinic, $P2_1/n$	monoclinic, $C2/c$
T [K]	123(2)	123(1)	123(1)	123(2)	126(3)	123(2)
a, b, c [Å]	9.1532(2), 33.9928(5), 14.0171(2)	11.8344(3), 13.0807(4), 14.2363(4)	9.6056(1), 16.9567(2), 14.3763(2)	9.5449(1), 15.9135(2), 15.1917(1)	13.6464(4), 12.1784(2), 28.7527(8)	25.4093(5), 19.3055(2), 15.7888(3)
α, β, γ [°]	90, 90.330(1), 90	67.789(3), 69.866(3), 77.591(2)	90, 92.825(1), 90	90, 94.664(1), 90	90, 90.183(2), 90	90, 126.781(3), 90
V [Å^3]	4361.25(13)	1906.47(11)	2338.76(5)	2299.87(4)	4778.4(2)	6203.2(3)
Z	8	3	4	4	8	8
F(000)	1792	816	1024	1024	2048	3124
Radiation	Cu-K_α	Cu-K_α	Cu-K_α	Cu-K_α	Cu-K_α	Cu-K_α
μ [mm^{-1}]	6.93	7.19	8.42	8.56	8.25	9.39
Habit	orange plate	red-brown block	green block	green plate	green rod	yellow plate
$T_{min.}$, $T_{max.}$	0.226, 0.677	0.296, 0.430	0.412, 0.655	0.317, 0.732	0.282, 0.824	0.382, 0.706
R_{int}	0.047	0.029	0.027	0.054	0.042	0.040
$(\sin \lambda/\theta)_{max}$ [Å^{-1}]	0.624	0.595	0.595	0.624	0.596	0.597
$R[F^2 > 2\sigma(F^2)]$, $wR(F^2)$, S	0.037, 0.106, 1.04	0.030, 0.079, 0.90	0.036, 0.097, 1.11	0.026, 0.069, 0.99	0.029, 0.055, 0.80	0.029, 0.075, 1.05
No. of reflections	8422	6639	7064	4626	8317	5508
$\Delta\rho_{max.}$, $\Delta\rho_{min.}$ [e Å^{-3}]	0.71, –0.47	0.44, –0.38	0.86, –0.33	0.49, –0.45	0.64, –0.31	0.97, –0.48

Table 4. Crystallographic data for **2**-I, **3**-Cl, **3**-Cl′, **3**-Br, **5**-Br, and **5**-I.

	2-I	**3**-Cl	**3**-Cl′	**3**-Br	**5**-Br	**5**-I
Formula	$C_{24}H_{39}Cu_2FeI_2NP_2$	$C_{18}H_{29}Cl_2Cu_2FeP_3$	$C_{18}H_{29}Cl_2Cu_2FeP_3$	$C_{18}H_{29}Br_2Cu_2FeP_3\cdot 0.15(C_7H_8)$	$C_{20}H_{35}Br_3Cu_3FeP_5\cdot 0.5(C_7H_8)$	$C_{20}H_{35}Cu_2FeI_2P_5$
FW	840.23	592.15	592.15	694.89	962.59	867.06
Crystal system, space group	orthorhombic, $P2_12_12_1$	monoclinic, $P2_1/c$	orthorhombic, $Pbca$	monoclinic, $P2_1/c$	triclinic, $P\bar{1}$	monoclinic, $P2_1/n$
T [K]	123(1)	123(2)	123(2)	123(2)	123(2)	123(1)
a, b, c [Å]	11.1640(2), 14.2254(2), 37.2743(4)	8.4412(1), 16.8393(2), 17.2062(2)	16.6294(3), 16.8479(3), 16.9793(3)	8.6057(1), 16.8865(1), 17.7057(1)	9.5046(2), 10.6841(2), 16.5146(2)	8.9909(3), 31.8655(12), 48.0476(18)
α, β, γ [°]	90, 90, 90	90, 100.823(1), 90	90, 90, 90	90, 99.799(1), 90	76.978(1), 78.518(1), 85.863(1)	90, 93.688(3), 90
V [Å^3]	5919.62(15)	2402.25(5)	4757.10(15)	2535.46(4)	1600.55(5)	13737.1(9)
Z	8	4	8	4	2	20
F(000)	3280	1200	2400	1374	946	8400
Radiation	Cu-K_α	Cu-K_α	Cu-K_α	Cu-K_α	Cu-K_α	Cu-K_α
μ [mm^{-1}]	23.04	10.77	10.21	11.95	12.61	26.43
Habit	yellow plate	red cube	red prism	purple prism	green prism	green-brown plate
$T_{min.}$, $T_{max.}$	0.055, 0.424	0.403, 0.562	0.189, 0.433	0.254, 0.433	0.212, 0.533	0.302, 0.669
R_{int}	0.042	0.049	0.034	0.028	0.021	0.115
$(\sin \lambda/\theta)_{max.}$ [Å^{-1}]	0.597	0.624	0.624	0.596	0.596	0.624
$R[F^2 > 2\sigma(F^2)]$, $wR(F^2)$, S	0.019, 0.047, 1.03	0.029, 0.074, 0.98	0.035, 0.088, 0.95	0.023, 0.054, 1.07	0.020, 0.049, 1.05	0.060, 0.148, 0.78
No. of reflections	10506	4828	4622	4485	5643	27095
$\Delta\rho_{max.}$, $\Delta\rho_{min.}$ [e Å^{-3}]	0.87, –0.62	0.41, –0.73	0.74, –0.65	0.58, –0.39	0.68, –0.45	1.92, –1.79

reason for this different coordination mode of CH_3CN cannot be given, but it may be attributable to the "outlier position" of CuI in coordination chemistry.[21] The coordination motif of $\{Cu_2(\mu\text{-}X)_2\}$ rings is known and has already been observed for several assemblies,[21] also with complexes of P_n ligands.[3,22]

Once crystallized, both compounds **2**-Br and **2**-I are insoluble in common solvents; therefore, characterization in solution could not be carried out. Only the slightly yellow-orange mother liquor could be used for NMR spectroscopic and mass spectrometric investigations. In the negative-ion ESI spectra only peaks assigned to copper halide fragments up to $[Cu_5Br_6]^-$ for **2**-Br and $[Cu_4I_5]^-$ for **2-I** were found. On the contrary, the positive-ion ESI spectra showed peaks for ferrocene-containing fragments with the largest at m/z = 1043.3 ($[\{Cp^*Fe(P_2C_3iPr_3)\}_2Cu_2Br]^+$) for **2**-Br and at m/z = 712.0 ($[\{Cp^*Fe(P_2C_3iPr_3)\}Cu_2I(CH_3CN)]^+$) for **2**-I. In the $^{31}P\{^1H\}$ NMR spectra of the mother liquors of **2**-Br and **2**-I, small singlets for the P_2C_3 ligand at δ = 14.3 and 15.9 ppm were observed, respectively. Since no significant broadening of the signal due to coordination of the P atoms to Cu (nuclear spin I = 3/2) is

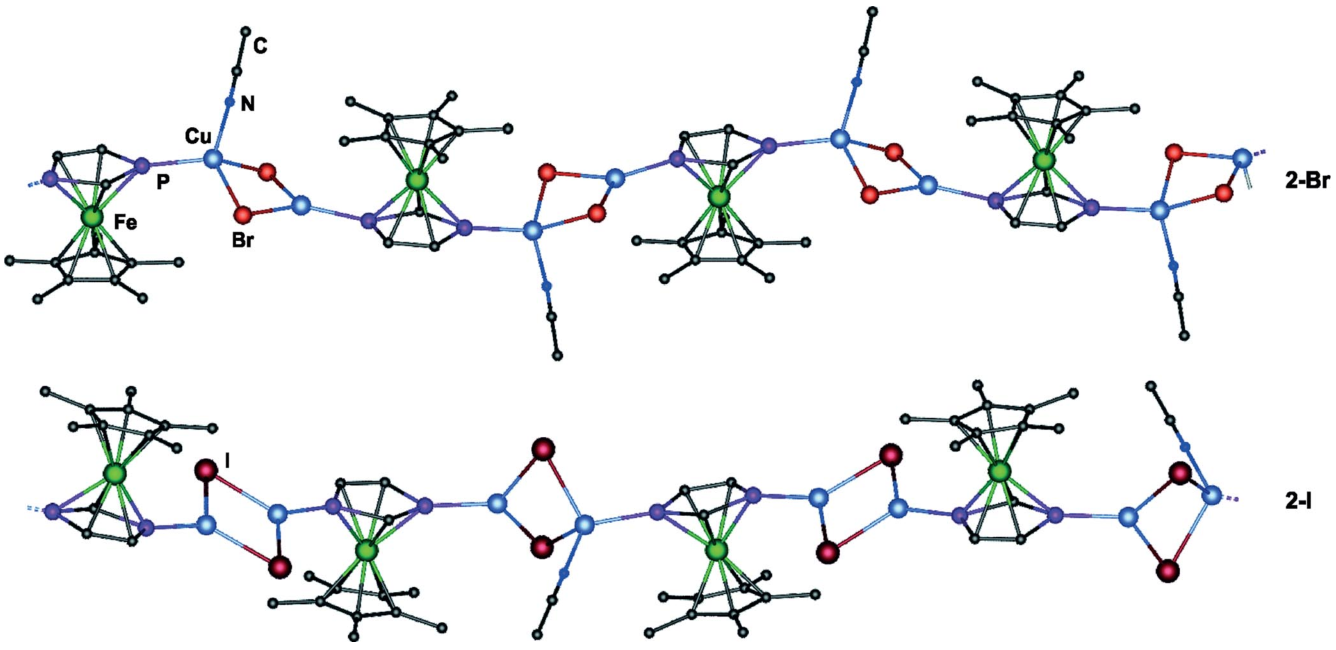

Figure 3. Section of the polymeric structures of **2**-Br and **2**-I. *i*Pr groups and H atoms are omitted for clarity.

recognizable, it can most likely be attributed to the free complex **2**.

Triphosphaferrocene 3 as Building Block

To study the influence of the smaller *i*Pr substituents in comparison to the Mes and *t*Bu derivatives, also the 1,2,4-triphosphaferrocene **3** was used for consecutive reactions. Layering experiments of **3** with CuX (X = Cl, Br) lead to the formation of the 2D polymeric compounds $[\{Cp^*Fe(\mu_4,\eta^{5:1:1:1}\text{-}P_3C_2iPr_2)\}Cu_2(\mu\text{-}Cl)_2]_n$ (**3**-Cl) and $[\{Cp^*Fe(\mu_4,\eta^{5:1:1:1}\text{-}P_3C_2iPr_2)\}Cu_2(\mu\text{-}Br)_2]_n\cdot 0.15n(C_7H_8)$ (**3**-Br), respectively (Scheme 4).

Both products crystallize as isomorphous compounds in the monoclinic space group $P2_1/c$ (crystallographic data: Table 4). In addition, compound **3**-Cl is polymorphous and also crystallizes in the orthorhombic space group *Pbca* (**3**-Cl′).

The X-ray structural analyses revealed 2D networks with a meshlike construction (Figure 4). Similar to **2**-X (X = Br, I), the phosphaferrocenes are linked by four-membered $\{Cu_2(\mu\text{-}X)_2\}$ rings (for bond lengths see Supporting Information). However,

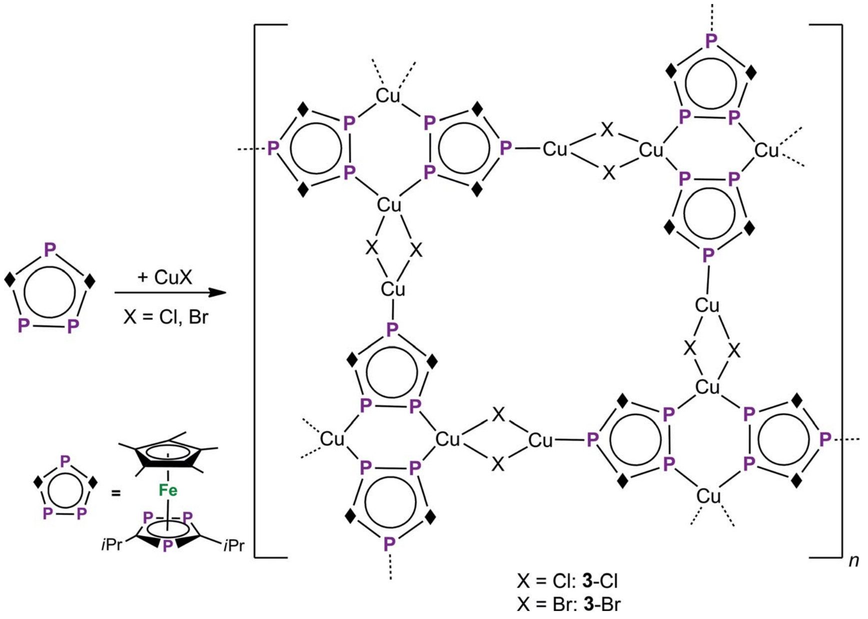

Scheme 4. 1,2,4-triphosphaferrocene-derived coordination polymers **3**-Cl and **3**-Br.

in **3**-Cl and **3**-Br the presence and coordination of three P atoms lead to extension of the polymer in two dimensions (Figure 4).

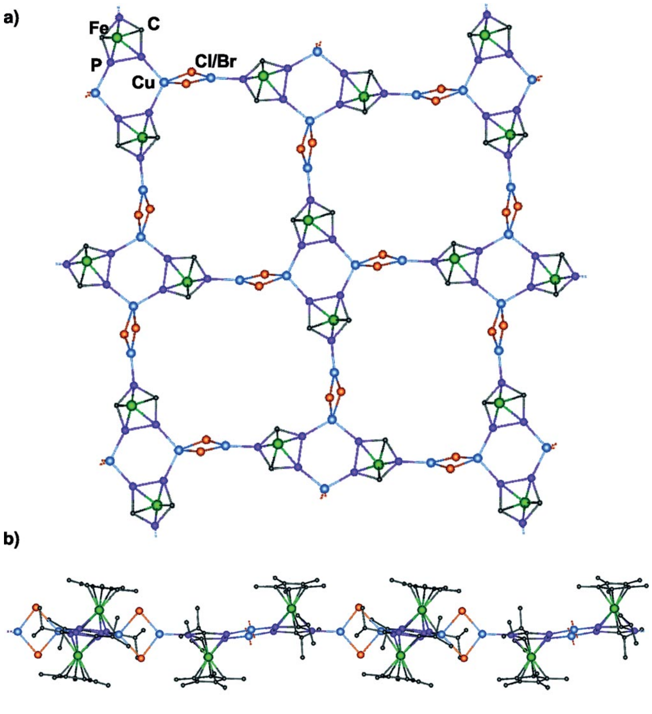

3-Cl/3-Br

Figure 4. Section of the polymeric structures of **3-Cl** and **3-Br**. a) Top view, Cp* and *i*Pr ligands are omitted for clarity. b) Side view, H atoms are omitted for clarity.

Notably, all copper ions attached to the isolated P atom of the P_3C_2 ring show a trigonal-planar environment, whereas any other Cu center is tetrahedrally coordinated. Again, adjacent phosphaferrocene units in **3**-Cl and **3**-Br are oriented upwards and downwards (Figure 4, b). The meshes therefore form layers separated by the Cp* ligands and, in the case of **3**-Br, provide enough space for a solvent molecule embedded between these layers.

Remarkably, **3**-Cl and **3**-Br are the first polymeric compounds containing triphosphaferrocenes and CuX (X = Cl, Br) despite many trials. Previous findings all demonstrate that fragmentation reactions of the phosphaferrocene occur[7,8] or dimeric[6a] and oligomeric[6b] compounds are formed. Only the use of CuI yields a coordination polymer in combination with $[\mathrm{Cp^*Fe}(\eta^5\text{-}\mathrm{P_3C_2}t\mathrm{Bu_2})]$.[6b] A meaningful comparison can be drawn to pentaphosphaferrocene-containing polymers bearing the *cyclo*-P_5 unit in a 1,2,4-coordination mode. This type is known for all halides in the 2D networks $[\{\mathrm{Cp^*Fe}(\mu_4,\eta^{5:1:1:1}\text{-}\mathrm{P_5})\}(\mathrm{CuX})]_n$ (X = Cl, Br, I). In these networks, the structural motif differs and the P atoms are linked by simple {CuX} units as opposed to $\{\mathrm{Cu_2}(\mu\text{-}\mathrm{X})_2\}$ (X = Cl, Br) rings in **3**-Cl and **3**-Br.

Since the 1D polymers **2**-Br and **2**-I are already insoluble, it is not surprising that also the 2D networks **3**-Cl and **3**-Br cannot be dissolved in any common solvent. Nonetheless, the mother liquors are still slightly colored, and hence they were analyzed by ESI mass spectrometry and $^{31}P\{^1H\}$ NMR spectroscopy. However, for **3**-Cl no signal in the respective NMR spectrum could be obtained, whereas in the $^{31}P\{^1H\}$ NMR spectrum of the mother liquor of **3**-Br small signals of the P_3C_2 ligand at δ = 11.4 ppm (d, $^2J_{PP}$ = 46 Hz, 2P) and δ = 22.7 ppm (t, $^2J_{PP}$ = 46 Hz, 1P) were observed, again most probably belonging to the free complex **3**. Similar to **2**-Br and **2**-I, in the negative-ion ESI mass spectra $[\mathrm{Cu}_{n-1}\mathrm{X}_n]^-$ units were detected with $n \leq 4$ for X = Cl and $n \leq 6$ for X = Br. The largest peaks in the positive-ion ESI spectra at *m/z* = 1541.4 and 1573.5 are assigned to $[\{\mathrm{Cp^*Fe}(\mathrm{P_3C_2}i\mathrm{Pr_2})\}_3\mathrm{Cu_4Cl_3}]^+$ and $[\{\mathrm{Cp^*Fe}(\mathrm{P_3C_2}i\mathrm{Pr_2})\}_2\mathrm{Cu_6Br_5}]^+$, respectively (for smaller fragments see Exp. Section).

Pentaphosphaferrocene 5 as Building Block

Since no supramolecular assemblies containing pentaphosphaferrocenes of the type $[(\eta^5\text{-}\mathrm{P_3C_2R_2})\mathrm{Fe}(\eta^5\text{-}\mathrm{P_2C_3R_3})]$ are mentioned in the literature, also the reactivity of **5** towards $\mathrm{Cu^I}$ halides was investigated. Diffusion experiments of solutions of **5** in CH_2Cl_2 or toluene and CuX (X = Br, I) in CH_3CN led to the formation of green prisms of $[\{(\mu_3,\eta^{5:1:1}\text{-}\mathrm{P_3C_2}i\mathrm{Pr_2})\mathrm{Fe}(\mu,\eta^{5:1}\text{-}\mathrm{P_2C_3}i\mathrm{Pr_3})\}\mathrm{Cu_3}(\mu\text{-Br})(\mu_3\text{-Br})(\mu_4\text{-Br})]_n{\cdot}0.5n(\mathrm{C_7H_8})$ (**5**-Br) and strongly intergrown plates of $[\{(\mu,\eta^{5:1}\text{-}\mathrm{P_3C_2}i\mathrm{Pr_2})\mathrm{Fe}(\mu,\eta^{5:1}\text{-}\mathrm{P_2C_3}i\mathrm{Pr_3})\}\mathrm{Cu_2}(\mu_3\text{-I})_2]_n$ (**5**-I), respectively (Scheme 5).

Due to the simpler structure, **5**-I is described first. It crystallizes in the monoclinic space group $P2_1/n$ and shows a 1D linear polymer formed by a {CuI} double strand with the sandwich complex **5** acting as a 1,1′-chelating ligand (Figure 5 right, for crystallographic details and bond lengths see Table 4 and Supporting Information). The regular structure of this ladder is formed by iodine atoms, all of which have a μ_3 coordination mode, and tetrahedrally coordinated Cu atoms.

The 1D polymer **5**-Br crystallizes as a solvate in the triclinic space group $P\bar{1}$ and shows a similar ladderlike scaffold (Table 4). The moieties of **5** also act as chelating ligands, though the coordination via three P atoms (two from the tri- and one from the diphospholyl ligand) leads to a 1,2,1′ connectivity. As a consequence, the {CuBr} double strand is bent at the positions of the triphospholyl ligand and a stairlike arrangement results with the bromide ligands in a μ, μ_3, or even μ_4 mode.

Similar structural motifs are already known for the hexaphosphaferrocene-containing polymers $[\{\mathrm{Fe}(\mu,\eta^{5:1}\text{-}\mathrm{P_3C_2}t\mathrm{Bu_2})_2\}\{\mathrm{Cu}(\mu_3\text{-X})\}_2]_x$ (X = Cl, Br, I) and $[\{\mathrm{Fe}(\mu,\eta^{5:1}\text{-}\mathrm{P_3C_2}t\mathrm{Bu_2})(\mu_3,\eta^{5:1:1}\text{-}\mathrm{P_3C_2}t\mathrm{Bu_2})\}\mathrm{Cu_3}(\mu\text{-I})(\mu_3\text{-I})_2(\mathrm{CH_3CN})]_x$.[23] In these compounds, the sterically demanding *t*Bu groups lead to a sinusoidal distortion of the strands, which is not the case for **5**-Br and **5**-I.

The characterization of the polymers **5**-Br and **5**-I in solution was again limited to the mother liquor. This time, only in the $^{31}P\{^1H\}$ NMR spectrum were signals corresponding to **5**-I observed, which can be assigned to the free complex **5**. Yet, they are slightly shifted to high field (δ = 9.5 ppm (s, 2 P, P_2C_3), 30.8 ppm (d, $^2J_{PP}$ = 43.2 Hz, 2 P, P_3C_2), 46.9 (t, $^2J_{PP}$ = 43.6 Hz, 1 P, P_3C_2). In the negative- and positive-ion ESI mass spectra of this solution, a variety of different fragments were detected (for details, see Exp. Section). Among them, the largest peak appears at *m/z* = 1078.3 for $[\mathrm{Cu_5I_6}]^-$ and 1796.9 for $[\{(\mathrm{P_2C_3}i\mathrm{Pr_2})\mathrm{Fe}(\mathrm{P_3C_2}i\mathrm{Pr_2})\}_2\mathrm{Cu_5I_4}]^+$, respectively.

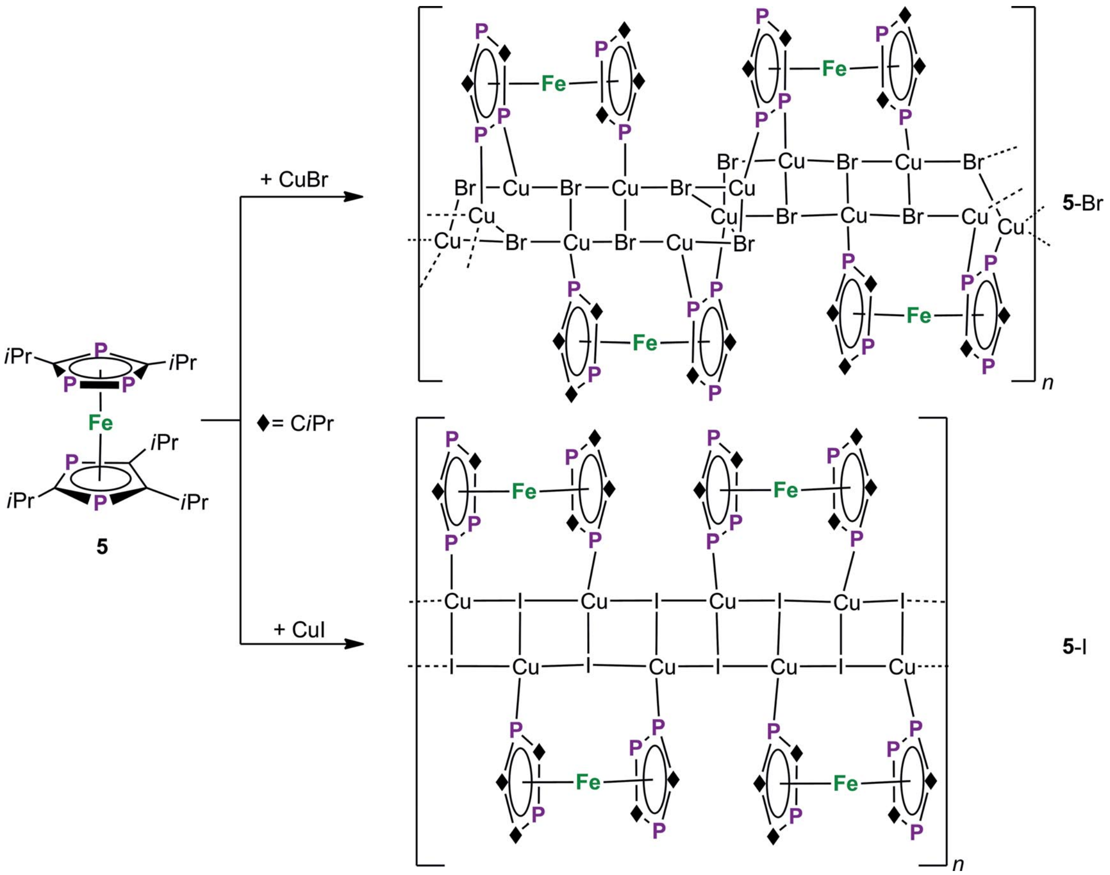

Scheme 5. 1,1′,2,3′,4-Pentaphosphaferrocene-derived coordination polymers **5-Br** and **5-I**.

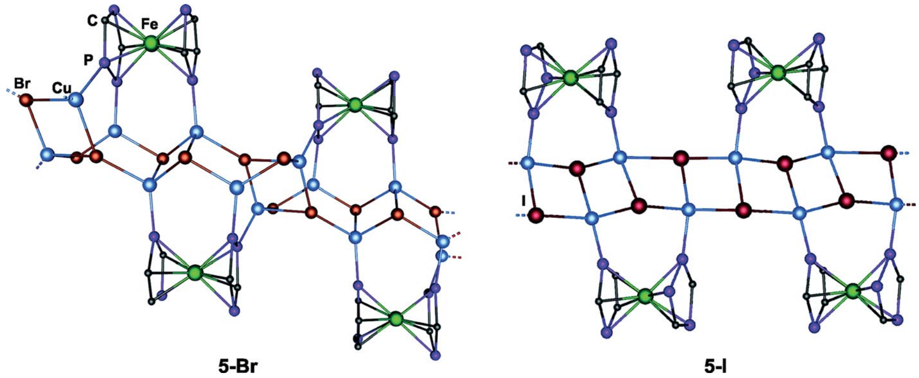

Figure 5. Section of the polymeric structures of **5-Br** (left) and **5-I** (right). *i*Pr groups and solvent molecules are omitted for clarity.

Conclusions

The di- and triphospholyl salts **1a**/**b** bearing rather small *i*Pr groups were synthesized starting from the phosphaalkene. By subsequent reaction with $FeBr_2$ and LiCp* a series of mainly novel phosphaferrocenes **2**–**6** containing two, three, four, five or six phosphorus atoms could be synthesized and isolated.

Since no supramolecular assemblies were known for a 1,3-diphospha- or 1,1′,2,3′,4-pentaphosphaferrocene, their coordination behavior towards Cu^I halides was studied. Both building blocks form 1D polymers, yet with different structures. Whereas with **2** as a ditopic linker infinite chains (**2**-Br, **2**-I) are obtained, the self-assembly of **5** with CuX (X = Br, I) leads to ladderlike structural motifs (**5**-Br, **5**-I) in which **5** acts as a chelating ligand. The obtained products are the first coordination polymers containing 1,3-di- and 1,1′,2,3′,4-pentaphosphaferrocenes, respectively.

Furthermore, previous results have shown that 1,2,4-triphosphaferrocenes tend to form di- and oligomeric products with intact sandwich complexes or polymeric products, albeit with fragmented and/or rearranged moieties of the building block. On the contrary, by using the *i*Pr-substituted compound **3**, isolation of 2D networks **3**-Cl and **3**-Br is possible. Hence, the additional phosphorus atom in combination with small *i*Pr substituents enables the phosphaferrocene **3** to act as tridentate planar linking unit that is predestined for the formation of 2D sheets. Both compounds contain intact units of **3** and therefore are the second and third representative of a triphosphaferrocene-based polymer. Furthermore, they show an unprecedented meshlike structure.

Experimental Section

General: All reactions were performed under an inert atmosphere of dry nitrogen or argon with standard vacuum, Schlenk, and glovebox techniques. Solvents were purified, dried, and degassed prior to use by standard procedures. $Me_3SiO(iPr)C{=}P(SiMe_3)$,[16] $K[P(SiMe_3)_2]$,[17] and $FeBr_2(dme)$[24] were synthesized according to the reported procedures. Commercially available chemicals were used without further purification. Solution NMR spectra were recorded with a Bruker Avance 300 or 400 spectrometer. The ESI-MS spectra were recorded with a ThermoQuest Finnigan MAT TSQ 7000 mass spectrometer, and EI-MS spectra were measured with a Finnigan MAT 95 mass spectrometer. Elemental analyses were performed with a Vario EL III apparatus.

Synthesis of 1a/b: A suspension of $K[P(SiMe_3)_2]$ (2.40 g, 0.11 mol) in a mixture of toluene (20 mL) and Et_2O (10 mL) was added to a solution of the phosphaalkene $Me_3SiO(iPr)C{=}P(SiMe_3)$ (5.5 g, 0.022 mol) in toluene (10 mL). An immediate color change from yellow to orange-red was observed. The reaction mixture was heated to 75 °C for 3 d. After cooling to room temp. the off-white powder was collected by filtration, washed with toluene (2 × 10 mL), and dried in vacuo to give **1a** and **1b** as a 1:1 mixture (1.35 g, 5.32 mmol, 48 %). Analytical data of **1a**: ^1H NMR ($[D_8]$thf): $\delta = 1.33$ (d, $^3J_{HH} = 6.8$ Hz, 12 H, CH_3-adjacent), 1.37 (d, $^3J_{HH} = 6.8$ Hz, 6 H, CH_3-isolated), 3.28 (m, 2 H, CH-adjacent), 3.44 (m, 1 H, CH-isolated) ppm. $^{31}P\{^1H\}$ NMR ($[D_8]$thf): $\delta = 161.44$ (s, 2 P) ppm. Analytical data of **1b**: ^1H NMR ($[D_8]$thf): $\delta = 1.43$ (d, $^3J_{HH} = 6.8$ Hz, 12 H, CH_3), 3.79 (m, 2 H, CH) ppm. $^{31}P\{^1H\}$ NMR ($[D_8]$thf): $\delta = 247.60$ (dd, $^2J_{PP} = 51.6$, 45.1 Hz, 1 P, $P_{isolated}$), 244.72 (pseudo-d, $^2J_{PP} = 49.0$ Hz, 2 P, $P_{adjacent}$) ppm.

Synthesis of Phosphaferrocenes 2–6: $FeBr_2(dme)$ (2.0 g, 6.5 mmol) and a mixture of **1a** and **1b** (1:1, 1.7 g, 6.5 mmol) were dissolved in thf (200 mL) at –40 °C. An immediate color change from yellow-orange to dark red occurred. A suspension of LiCp* (930 mg, 6.5 mmol) in thf (50 mL) was added subsequently. The reaction mixture was warmed to room temp. and the solvent removed under reduced pressure. Afterwards, the residue was dissolved in toluene, the solution filtered through Celite, and the solvent again removed. The solid was adsorbed on silica and loaded onto a column filled with silica (50 cm × 3 cm). By using hexane as eluent, a yellow band of $[Cp^*{}_2Fe]$ could be eluted, followed by a green fraction containing the hexaphosphaferrocene **6**, the pentaphosphaferrocene **5**, and the tetraphosphaferrocene **4** (70 mg, ca. 3 %, calculated by means of the average molar weight). By switching to a hexane/toluene mixture (10:1) a red band of the triphosphaferrocene **3** and the diphosphaferrocene **2** (440 mg, ca. 17 %, calculated by means of the average molar weight) could be eluted. To separate **2** and **3** or **4**, **5**, and **6**, the solvent of the respective fraction must be removed and a further chromatographic workup is needed (50 cm × 3 cm). Unfortunately, the products cannot be eluted as separate bands with hexane as eluent; therefore, several fractions must be collected. The first fraction gives pure **2**, the last pure **3**, and the intermediate ones give mixtures with different molar ratios (for an NMR spectrum, see the Supporting Information). Furthermore, elemental analysis could not be carried out, since the phosphaferrocenes are oily solids at room temp. and crystals obtained at lower temperature start melting when warmed to room temp. Therefore, standard solutions were prepared for following reactions.

Analytical Data of 2/3: Yield: 440 mg (17 %): integral ratios from $^{31}P\{^1H\}$ NMR (C_6D_6): 50 % **2**, 50 % **3**. Analytical data of **2**: ^1H NMR (C_6D_6): $\delta = 1.16$ (d, $^3J_{HH} = 6.1$ Hz, 6 H, *i*Pr-CH_3), 1.24 (d, $^3J_{HH} = 6.2$ Hz, 6 H, *i*Pr-CH_3), 1.60 (d, $^3J_{HH} = 6.2$ Hz, 6 H, *i*Pr-CH_3), 1.70 (s, 15 H, Cp*-CH_3), 2.26 (br. m, 1 H, *i*Pr-CH), 2.38 (br. m, 2 H, *i*Pr-CH) ppm. $^{31}P\{^1H\}$ NMR (C_6D_6): $\delta = -2.84$ (s, P_2C_3) ppm. FD-MS (toluene): 418.2 (M^+). Analytical data of **3**: ^1H NMR (C_6D_6): $\delta = 1.32$ (d, $^3J_{HH} = 6.6$ Hz, 6 H, *i*Pr-CH_3), 1.43 (d, $^3J_{HH} = 6.5$ Hz, 6 H, *i*Pr-CH_3), 1.62 (s, 15 H, Cp*-CH_3), 2.72 (br. m, 2 H, *i*Pr-CH) ppm. $^{31}P\{^1H\}$ NMR (C_6D_6): $\delta = 29.69$ (t, $^2J_{PP} = 43.8$ Hz, 1 P, $P_{isolated}$), 49.63 (d, $^2J_{PP} = 43.8$ Hz, 2 P, $P_{adjacent}$) ppm. FD-MS (toluene): 394.3 (M^+). Analytical data of **4**/**5**/**6**: Yield: 70 mg: integral ratios from $^{31}P\{^1H\}$ NMR (C_6D_6): 57 % **5**, 39 % **6** and 4 % **4**. Analytical data of **4**: $^{31}P\{^1H\}$ NMR (C_6D_6): $\delta = 6.7$ (br. s, 4 P) ppm. FD-MS (hexane): 510.2 (M^+). Analytical data of of **5**: ^1H NMR (C_6D_6): $\delta = 1.04$ (d, $^3J_{HH} = 6.7$ Hz, 6 H, *i*Pr-CH_3), 1.23 (d, $^3J_{HH} = 6.7$ Hz, 6 H, *i*Pr-CH_3), 1.45 (d, $^3J_{HH} = 6.7$ Hz, 6 H, *i*Pr-CH_3), 1.54 (d, $^3J_{HH} = 6.7$ Hz, 6 H, *i*Pr-CH_3), 1.72 (d, $^3J_{HH} = 6.7$ Hz, 6 H, *i*Pr-CH_3), 2.46 (br. m, 2 H, *i*Pr-CH), 2.59 (br. m, 1 H, *i*Pr-CH), 3.12 (br. m, 2 H, *i*Pr-CH) ppm. $^{31}P\{^1H\}$ NMR (C_6D_6): $\delta = 15.00$ (s, 2 P, P_2C_3), 46.90 (t, $^2J_{PP} = 42.0$ Hz, 1 P, $P_{isolated}$), 53.68 (d, $^2J_{PP} = 42.0$ Hz, 2 P, $P_{adjacent}$) ppm. FD-MS (hexane): 486.1 (M^+). Analytical data of **6**: ^1H NMR (C_6D_6): $\delta = 1.29$ (d, $^3J_{HH} = 6.7$ Hz, 12 H, *i*Pr-CH_3), 1.36 (d, $^3J_{HH} = 6.7$ Hz, 12 H, *i*Pr-CH_3), 2.91 (br. m, 4 H, *i*Pr-CH) ppm. $^{31}P\{^1H\}$ NMR (C_6D_6): $\delta = 51.3$ (br. m, 2 P, $P_{adjacent}$), 68.7 (br. m, 1 P, $P_{isolated}$) ppm. $^{31}P\{^1H\}$ NMR (CD_2Cl_2, 193K): $\delta = 46.22$ (d, $^2J_{PP} = 34$ Hz, 2 P, $P_{adjacent}$), 69.28 (t, $^2J_{PP} = 38$ Hz, 1 P, $P_{isolated}$) ppm. FD-MS (hexane): 462.0 (M^+).

Synthesis of 2-Br: A solution of CuBr (24 mg, 0.16 mmol) in acetonitrile (1 mL) was layered on a solution of **2** (35 mg, 0.08 mmol) in toluene (0.5 mL) in a narrow Schlenk tube. After diffusion, small orange platelets of **2**-Br had formed. The mother liquor was decanted and the crystals were washed with CH_2Cl_2 and then dried under vacuum (5 mg, 6.7 µmol, 8 %). Analytical data of **2**-Br: $^{31}P\{^1H\}$ NMR (C_6D_6 capillary, mother liquor): $\delta = 14.26$ (s, P_2C_3) ppm. Positive-ion ESI-MS (mother liquor, toluene/CH_3CN): *m/z* (%) = 1043.3 $[\{Cp^*Fe(P_2C_3iPr_3)\}_2Cu_2Br]^+$, 899.3 $[\{Cp^*Fe(P_2C_3iPr_3)\}_2Cu]^+$, 326.1 (100) $[Cp^*{}_2Fe]^+$. Negative-ion ESI-MS (mother liquor, toluene/CH_3CN): *m/z* (%) = 798.3 $[Cu_5Br_6]^-$, 652.4 $[Cu_4Br_5]^-$, 510.4 $[Cu_3Br_4]^-$, 366.5 (100) $[Cu_2Br_3]^-$, 222.7 $[CuBr_2]^-$. $[\{Cp^*Fe(\eta^5\text{-}P_2C_3iPr_3)\}Cu_2Br_2(CH_3CN)_{1.5}]$ (766.8 g/mol): calcd. C 39.16, H 5.32, N 2.74; found C 39.38, H 5.43, N 2.59.

Synthesis of 2-I: A solution of CuI (32 mg, 0.17 mmol) in acetonitrile (6 mL) was layered on a solution of **2** (35 mg, 0.08 mmol) in toluene (3 mL) in a narrow Schlenk tube. After diffusion, small orange platelets of **2**-I had formed. The mother liquor was decanted and the crystals were washed with CH_2Cl_2 and then dried under vacuum (7 mg, 8.8 µmol, 10 %). Analytical data of **2**-I: $^{31}P\{^1H\}$ NMR (C_6D_6 capillary, mother liquor): $\delta = 15.95$ (s, P_2C_3) ppm. Positive-ion ESI-MS (mother liquor, toluene/CH_3CN): *m/z* (%) = 712.0 $[\{Cp^*Fe(P_2C_3iPr_3)\}Cu_2I(CH_3CN)]^+$, 522.1 $[\{Cp^*Fe(P_2C_3iPr_3)\}Cu(CH_3CN)]^+$, 326.1 (100) $[Cp^*{}_2Fe]^+$. Negative-ion ESI-MS (mother liquor, toluene/CH_3CN): *m/z* (%) = 888.4 $[Cu_4I_5]^-$, 698.5 $[Cu_3I_4]^-$, 506.6 $[Cu_2I_3]^-$, 316.6 (100) $[CuI_2]^-$. $[\{Cp^*Fe(\eta^5\text{-}P_2C_3iPr_3)\}Cu_2I_2]$ (799.2 g/mol): calcd. C 33.06, H 4.54; found C 33.76, H 4.63.

Synthesis of 3-Cl: A colorless solution of CuCl (30 mg, 0.30 mmol) in acetonitrile (3 mL) was layered on a red solution of **3** (36 mg, 0.09 mmol) in toluene (2 mL) in a narrow Schlenk tube. Thereby, the phase boundary turned orange and overnight small orange crystals of **3**-Cl formed. After complete diffusion, the mother liquor was decanted and the crystals were washed with hexane/toluene (3:1, 3 × 3 mL) and then dried under vacuum (17 mg, 0.03 mmol, 33 %). Analytical data of **3**-Cl: $^{31}P\{^1H\}$ NMR (C_6D_6 capillary, mother liquor): no signal detectable. Positive-ion ESI-MS (mother liquor, toluene/CH_3CN): m/z = 1541.4 $[\{Cp^*Fe(P_3C_2iPr_2)\}_3Cu_4Cl_3]^+$, 1441.4 $[\{Cp^*Fe(P_3C_2iPr_2)\}_3Cu_3Cl_2]^+$, 1384.4 $[\{Cp^*Fe(P_3C_2iPr_2)\}_3Cu_2Cl(CH_3CN)]^+$, 1341.7 $[\{Cp^*Fe(P_3C_2iPr_2)\}_3Cu_2Cl]^+$, 1541.4 $[\{Cp^*Fe(P_3C_2iPr_2)\}_3Cu_4Cl_3]^+$. Negative-ion ESI-MS (mother liquor, toluene/CH_3CN): m/z (%) = 332.5 (5) $[Cu_3Cl_4]^-$, 232.7 (100) $[Cu_2Cl_3]^-$, 134.7 (20) $[CuCl_2]^-$. $[\{Cp^*Fe(\eta^5\text{-}P_3C_2iPr_2)\}Cu_2Cl_2]$ (592.2 g/mol): calcd. C 36.51, H 4.94; found C 37.51, H 5.03.

Synthesis of 3-Br: A colorless solution of CuBr (40 mg, 0.28 mmol) in acetonitrile (3 mL) was layered on a red solution of **3** (36 mg, 0.09 mmol) in toluene (2 mL) in a narrow Schlenk tube. Thereby, the phase boundary turned orange and overnight a colorless precipitate formed. Within a week, small orange crystals of **3**-Br had formed. The mother liquor was decanted and the crystals were washed with hexane/toluene (3:1, 3 × 3 mL) and CH_3CN to remove precipitated CuBr and then dried under vacuum (27 mg, 0.04 mmol, 44 %). Analytical data of **3**-Br: $^{31}P\{^1H\}$ NMR (C_6D_6 capillary, mother liquor): δ = 11.38 (d, $^2J_{PP}$ = 46 Hz, 2 P, $P_{adjacent}$), 22.71 (t, $^2J_{PP}$ = 46 Hz, 1 P, $P_{isolated}$) ppm. Positive-ion ESI-MS (mother liquor, toluene/CH_3CN): m/z = 1573.5 $[\{Cp^*Fe(P_3C_2iPr_2)\}_2Cu_6Br_5]^+$, 1507.6 $[\{Cp^*Fe(P_3C_2iPr_2)\}Cu_8Br_7(CH_3CN)]^+$, 1431.4 $[\{Cp^*Fe(P_3C_2iPr_2)\}_2Cu_5Br_4]^+$, 1356.6 $[\{Cp^*Fe(P_3C_2iPr_2)\}Cu_7Br_6(CH_3CN)]^+$, 1283.4 $[\{Cp^*Fe(P_3C_2iPr_2)\}_2Cu_4Br_3]^+$, 1209.6 $[\{Cp^*Fe(P_3C_2iPr_2)\}Cu_6Br_5(CH_3CN)]^+$, 1135.5 $[\{Cp^*Fe(P_3C_2iPr_2)\}_2Cu_3Br_2]^+$, 985.3 $[\{Cp^*Fe(P_3C_2iPr_2)\}_2Cu_2Br]^+$. Negative-ion ESI-MS (mother liquor, toluene/CH_3CN): m/z (%) = 798.1 (3) $[Cu_5Br_6]^-$, 654.2 (3) $[Cu_4Br_5]^-$, 510.4 (18) $[Cu_3Br_4]^-$, 366.3 (100) $[Cu_2Br_3]^-$, 222.5 (42) $[CuBr_2]^-$. $[\{Cp^*Fe(\eta^5\text{-}P_3C_2iPr_2)\}Cu_2Br_2(CH_3CN)_{0.1}(C_7H_8)_{0.1}]$ (694.4 g/mol): calcd. C 32.69, H 4.37, N 0.20; found C 32.84, H 4.29, N 0.3.

Synthesis of 5-Br: A colorless solution of CuBr (34 mg, 0.24 mmol) in acetonitrile (3 mL) was layered on a green solution of **5** (23 mg, 0.05 mmol) in CH_2Cl_2 (3 mL) in a narrow Schlenk tube. Thereby, no significant color change at the phase boundary could be observed. After diffusion, the reaction mixture was again layered with toluene. Within a few days, green prisms of **5**-Br formed. The mother liquor was decanted and the crystals were washed with hexane (3 × 3 mL) and dried in vacuo (24 mg, 0.025 mmol, 50 %). Analytical data of **5**-Br: $^{31}P\{^1H\}$ NMR (mother liquor, C_6D_6 capillary): no signal detectable. Negative-ion ESI-MS (mother liquor, CH_2Cl_2/CH_3CN): m/z (%) = 510.4 (15) $[Cu_3Br_4]^-$, 366.4 (100) $[Cu_2Br_3]^-$, 222.5 (37) $[CuBr_2]^-$. $[\{(\eta^5\text{-}P_3C_2iPr_2)Fe(\eta^5\text{-}P_2C_3iPr_3)\}Cu_3Br_3(C_7H_8)_{0.5}]$ (962.7 g/mol): calcd. C 29.32, H 4.08; found C 29.46, H 4.11.

Synthesis of 5-I: A colorless solution of CuI (45 mg, 0.24 mmol) in acetonitrile (3 mL) was layered on a green solution of **5** (23 mg, 0.05 mmol) in CH_2Cl_2 (3 mL) in a very narrow Schlenk tube. Thereby, no significant color change at the phase boundary could be observed. Within two weeks, green-brown intergrown plates of **5**-I formed. The mother liquor was decanted and the crystals were washed with hexane (3 × 3 mL) and dried in vacuo (16 mg, 0.018 mmol, 37 %). Analytical data of **5**-I: $^{31}P\{^1H\}$ NMR (mother liquor, C_6D_6 capillary): δ = 9.45 (s, 2 P, P_2C_3), 30.75 (d, $^2J_{PP}$ = 43.2 Hz, 2 P, $P_{adjacent}$), 46.88 (t, $^2J_{PP}$ = 43.6 Hz, 1 P, $P_{isolated}$) ppm. Positive-ion ESI-MS (mother liquor, CH_2Cl_2/CH_3CN): m/z (%) = 1796.9 $[\{(P_2C_3iPr_2)Fe(P_3C_2iPr_2)\}_2Cu_5I_4]^+$, 1690.2 $[\{(P_2C_3iPr_2)Fe(P_3C_2iPr_2)\}Cu_7I_6]^+$, 1628.8 $[\{(P_2C_3iPr_2)Fe(P_3C_2iPr_2)\}Cu_6I_5(CH_3CN)(CH_2Cl_2)]^+$, 1587.9 $[\{(P_2C_3iPr_2)Fe(P_3C_2iPr_2)\}Cu_6I_5(CH_2Cl_2)]^+$, 1606.9 $[\{(P_2C_3iPr_2)Fe(P_3C_2iPr_2)\}_2Cu_4I_3]^+$, 1543.9 $[\{(P_2C_3iPr_2)Fe(P_3C_2iPr_2)\}Cu_6I_5(CH_3CN)]^+$, 1500.6 $[\{(P_2C_3iPr_2)Fe(P_3C_2iPr_2)\}Cu_6I_5]^+$, 1437.2 $[\{(P_2C_3iPr_2)Fe(P_3C_2iPr_2)\}Cu_5I_4(CH_3CN)_3]^+$, 1417.1 $[\{(P_2C_3iPr_2)Fe(P_3C_2iPr_2)\}_2Cu_3I_2]^+$, 1395.9 $[\{(P_2C_3iPr_2)Fe(P_3C_2iPr_2)\}Cu_5I_4(CH_3CN)_2]^+$, 1288.2 $[\{(P_2C_3iPr_2)Fe(P_3C_2iPr_2)\}Cu_4I_3(CH_2Cl_2)_2]^+$, 1247.1 $[\{(P_2C_3iPr_2)Fe(P_3C_2iPr_2)\}Cu_4I_3(CH_3CN)(CH_2Cl_2)]^+$, 1227.1 $[\{(P_2C_3iPr_2)Fe(P_3C_2iPr_2)\}_2Cu_2I_1]^+$, 1206.1 $[\{(P_2C_3iPr_2)Fe(P_3C_2iPr_2)\}Cu_4I_3(CH_2Cl_2)]^+$, 1120.6 $[\{(P_2C_3iPr_2)Fe(P_3C_2iPr_2)\}Cu_4I_3]^+$. Negative ion ESI-MS (mother liquor, CH_2Cl_2/CH_3CN): m/z (%) = 1078.3 (8) $[Cu_5I_6]^-$, 888.4 (14) $[Cu_4I_5]^-$, 698.4 (47) $[Cu_3I_4]^-$, 506.5 (78) $[Cu_2I_3]^-$, 316.6 (100) $[CuI_2]^-$. $[\{(\eta^5\text{-}P_3C_2iPr_2)Fe(\eta^5\text{-}P_2C_3iPr_3)\}Cu_2I_2]$ (867.1 g/mol): calcd. C 27.70, H 4.07; found C 27.78, H 4.02.

Supporting Information (see footnote on the first page of this article): Supporting information for this article (details on the diffraction experiments including tables of bond lengths) is given via a link at the end of the document.

CCDC-1415107 (for **2**), -1415108 (for **4**), -1415109 (for **5**), -1415110 (for **5′**), -1415111 (for **5′′**), -1415112 (for **2**-Br), -1415113 (for **2**-I), -1415115 (for **3**-Cl), -1415114 (for **3**-Cl′), -1415116 (for **3**-Br), -1415117 (for **5**-Br) and -1415118 (for **5**-I) contain the supplementary crystallographic data for this paper. These data can be obtained free of charge from The Cambridge Crystallographic Data Centre via www.ccdc.cam.ac.uk/data_request/cif.

Acknowledgments

This work was supported by the Deutsche Forschungsgemeinschaft (DFG). C. H. is grateful for a PhD fellowship of the Fonds der Chemischen Industrie. The European Research Council (ERC) is acknowledged for the support in the SELFPHOS AdG-2013-339072 project.

Keywords: Supramolecular chemistry · Self-assembly · Polymers · Phosphaferrocenes · Copper

[1] G. Maerkl, *Angew. Chem.* **1966**, *78*, 907–908.
[2] L. Weber, *Angew. Chem. Int. Ed.* **2002**, *41*, 563–572; *Angew. Chem.* **2002**, *114*, 583.
[3] J. Bai, A. V. Virovets, M. Scheer, *Angew. Chem. Int. Ed.* **2002**, *41*, 1737–1740; *Angew. Chem.* **2002**, *114*, 1808.
[4] a) C. Schwarzmaier, A. Schindler, C. Heindl, S. Scheuermayer, E. V. Peresypkina, A. V. Virovets, M. Neumeier, R. Gschwind, M. Scheer, *Angew. Chem. Int. Ed.* **2013**, *52*, 10896–10899; b) J. Bai, A. V. Virovets, M. Scheer, *Science* **2003**, *300*, 781–783.
[5] a) C. Heindl, A. Schindler, M. Bodensteiner, E. V. Peresypkina, A. V. Virovets, M. Scheer, *Phosphorus Sulfur Silicon Relat. Elem.* **2015**, *190*, 397–403; b) M. M. Al-Ktaifani, P. B. Hitchcock, J. F. Nixon, *J. Organomet. Chem.* **2008**, *693*, 611–618; c) M. Scheer, S. Deng, O. J. Scherer, M. Sierka, *Angew. Chem. Int. Ed.* **2005**, *44*, 3755–3758; *Angew. Chem.* **2005**, *117*, 3821; d) C. S. J. Callaghan, P. B. Hitchcock, J. F. Nixon, *J. Organomet. Chem.* **1999**, *584*, 87–93; e) M. H. A. Benvenutti, P. B. Hitchcock, J. F. Nixon, M. D. Vargas, *Chem. Commun.* **1996**, 441–443; f) C. Müller, R. Bartsch, A. Fischer, P. G. Jones, R. Schmutzler, *J. Organomet. Chem.* **1996**, *512*, 141; g) M. H. A. Benvenutti, P. B. Hitchcock, J. F. Nixon, M. D. Vargas, *J. Chem. Soc., Dalton Trans.* **1996**, 739–746; h) C. Mueller, R. Bartsch, A. Fischer, P. G. Jones, *Polyhedron* **1993**, *12*, 1383–1390; i) C. Müller, R. Bartsch, A. Fischer, P. G. Jones, *J. Organomet. Chem.* **1993**, *453*, C16; j) R. Bartsch, A. Gelessus, J. F. Nixon, P. B. Hitchcock, *J. Organomet. Chem.* **1992**, *430*, C10; k) R. Bartsch, P. B. Hitchcock, J. F. Nixon, *J. Organomet. Chem.* **1988**, *340*, C37–C39.
[6] a) S. Deng, C. Schwarzmaier, M. Zabel, J. F. Nixon, M. Bodensteiner, E. V. Peresypkina, G. Balazs, M. Scheer, *Eur. J. Inorg. Chem.* **2011**, 2991–3001; b) A. Schindler, G. Balazs, M. Zabel, C. Groeger, R. Kalbitzer, M. Scheer, *C. R. Chim.* **2010**, *13*, 1241–1248.
[7] S. Deng, C. Schwarzmaier, U. Vogel, M. Zabel, J. F. Nixon, M. Scheer, *Eur. J. Inorg. Chem.* **2008**, 4870–4874.

[8] C. Heindl, A. Kuntz, E. V. Peresypkina, A. V. Virovets, M. Zabel, D. Luedeker, G. Brunklaus, M. Scheer, *Dalton Trans.* **2015**, *44*, 6502–6509.

[9] R. Bartsch, J. F. Nixon, *J. Organomet. Chem.* **1991**, *415*, C15–18.

[10] N. Maigrot, L. Ricard, C. Charrier, F. Mathey, *Angew. Chem. Int. Ed. Engl.* **1990**, *29*, 534–535; *Angew. Chem.* **1990**, *102*, 575.

[11] a) N. Maigrot, M. L. Sierra, C. Charrier, L. Ricard, F. Mathey, *Polyhedron* **1992**, *11*, 601–606; b) M. L. Sierra, N. Maigrot, C. Charrier, L. Ricard, F. Mathey, *Organometallics* **1992**, *11*, 459–462.

[12] a) R. Bartsch, P. B. Hitchcock, J. F. Nixon, *J. Chem. Soc., Chem. Commun.* **1987**, 1146–1148; b) M. Driess, D. Hu, H. Pritzkow, H. Schaeufele, U. Zenneck, M. Regitz, W. Roesch, *J. Organomet. Chem.* **1987**, *334*, C35–C38.

[13] R. Bartsch, A. Gelessus, P. B. Hitchcock, J. F. Nixon, *J. Organomet. Chem.* **1992**, *430*, C10–C14.

[14] D. Boehm, F. Heinemann, D. Hu, S. Kummer, U. Zenneck, *Collect. Czech. Chem. Commun.* **1997**, *62*, 309–317.

[15] G. Becker, W. Becker, R. Knebl, H. Schmidt, U. Weeber, M. Westerhausen, *Nova Acta Leopold.* **1985**, *59*, 55–67.

[16] W. Roesch, U. Vogelbacher, T. Allspach, M. Regitz, *J. Organomet. Chem.* **1986**, *306*, 39–53.

[17] F. Uhlig, R. Hummeltenberg, *J. Organomet. Chem.* **1993**, *452*, C9–C10.

[18] D. Heift, Z. Benko, H. Gruetzmacher, *Chem. Eur. J.* **2014**, *20*, 11326–11330.

[19] a) M. Tanabe, I. Manners, *J. Am. Chem. Soc.* **2004**, *126*, 11434–11435; b) T. Mizuta, Y. Imamura, K. Miyoshi, *J. Am. Chem. Soc.* **2003**, *125*, 2068–2069.

[20] a) P. Pyykkö, M. Atsumi, *Chem. Eur. J.* **2009**, *15*, 12770–12779; b) P. Pyykkö, M. Atsumi, *Chem. Eur. J.* **2009**, *15*, 186–197.

[21] R. Peng, M. Li, D. Li, *Coord. Chem. Rev.* **2010**, *254*, 1–18.

[22] M. Scheer, *Dalton Trans.* **2008**, 4372–4386.

[23] A. Schindler, M. Zabel, J. F. Nixon, M. Scheer, *Z. Naturforsch. B* **2009**, *64*, 1429–1437.

[24] S. Deng, *Diploma thesis*, University of Karlsruhe, Germany, **2002**.

Received: August 4, 2015